Available online at www.sciencedirect.com
SCIENCE DIRECT®
ELSEVIER
Nuclear Instruments and Methods in Physics Research A 518 (2004) 244–248
NUCLEAR INSTRUMENTS & METHODS IN PHYSICS RESEARCH Section A
www.elsevier.com/locate/nima

Production and detection of cold antihydrogen atoms

M. Amoretti[a,*], C. Amsler[b], G. Bonomi[c], A. Bouchta[c], P.D. Bowe[d], C. Carraro[a,e], C.L. Cesar[f], M. Charlton[g], M. Doser[c], V. Filippini[h], A. Fontana[h,i], M.C. Fujiwara[j], R. Funakoshi[j], P. Genova[h,i], J.S. Hangst[d], R.S. Hayano[j], L.V. Jørgensen[g], V. Lagomarsino[a,e], R. Landua[c], D. Lindelöf[b], E. Lodi Rizzini[k], M. Macrí[a], N. Madsen[b], G. Manuzio[a,e], P. Montagna[h,i], H. Pruys[b], C. Regenfus[b], A. Rotondi[h,i], G. Testera[a], A. Variola[a], D.P. van der Werf[g]

[a] *Istituto Nazionale di Fisica Nucleare, Sezione di Genova, Genova 16146, Italy*
[b] *Physik-Institut, Zürich University, CH-8057 Zürich, Switzerland*
[c] *EP Division, CERN, CH-1211 Geneva 23, Switzerland*
[d] *Department of Physics and Astronomy, University of Aarhus, DK-8000 Aarhus C, Denmark*
[e] *Dipartimento di Fisica, Università di Genova, Genova 16146, Italy*
[f] *Instituto de Fisica, Universidade Federal do Rio de Janeiro, Rio de Janeiro 21945-970, and Centro Federal de Educação Tecnologica do Ceara, Fortaleza 60040-531, Brazil*
[g] *Department of Physics, University of Wales Swansea, Swansea SA2 8PP, UK*
[h] *Istituto Nazionale di Fisica Nucleare, Sezione di Pavia, Pavia 27100, Italy*
[i] *Dipartimento di Fisica Nucleare e Teorica, Università di Pavia, Pavia 27100, Italy*
[j] *Department of Physics, University of Tokyo, Tokyo 113-0033, Japan*
[k] *Dipartimento di Chimica e Fisica per l'Ingegneria e per i Materiali, Università di Brescia; Istituto Nazionale di Fisica Nucleare, Gruppo collegato di Brescia, Brescia 25123, Italy*

For the ATHENA Collaboration

Abstract

The production and observation of cold antihydrogen atoms have been recently reported by the ATHENA experiment at the CERN Antiproton Decelerator. The antiatoms were produced by mixing low-energy antiprotons and positrons in an electromagnetic trap. The antihydrogen detection is based on the observation of a characteristic signature in the annihilation of the neutral antiatoms on the trap walls by means of an imaging particle detector. An overview of the apparatus is given and the results obtained are discussed.

PACS: 11.30.Er; 36.10.−k; 52.27.Jt

Keywords: Antihydrogen; Fundamental symmetrics; CPT invariance; Antiprotons; Positrons; Non-neutral plasmas

*Corresponding author.
E-mail address: marco.amoretti@ge.infn.it (M. Amoretti).

0168-9002/$ - see front matter © 2003 Elsevier B.V. All rights reserved.
doi:10.1016/j.nima.2003.10.072

1. Introduction

The ATHENA collaboration recently produced and detected cold antihydrogen atoms [1] at the CERN Antiproton Decelerator (AD) [2]. A similar result has been subsequently reported by the ATRAP collaboration [3]. The production of a considerable amount of cold antihydrogen atoms is a fundamental milestone on the road to a high-precision comparison of the interaction of hydrogen and antihydrogen with electromagnetic and gravitational fields [4].

2. Antihydrogen production

The ATHENA apparatus consists of three main electromagnetic traps for charged particles: the trap used to catch and cool the antiprotons, the positron accumulator, and the trap for the particles mixing located in the middle between the previous two traps (see Fig. 1). The antiproton and the mixing trap are placed inside an ultra-high vacuum cryostat immersed in a 3 T superconducting magnetic field. The positron accumulation trap is located inside a room temperature vacuum chamber in a 0.14 T magnetic field. An imaging particle detector [5], used for the identification of the antihydrogen annihilation products, surrounds the mixing trap (Fig. 2(a)).

The antiproton capture trap is a multi-electrode cylindrical Penning–Malmberg trap in which antiprotons supplied by the AD are trapped in a high voltage potential well ($\sim$5 kV), after being slowed down by means of several degrader foils. These trapped antiprotons are cooled by collisional interaction with preloaded electrons, which in turn self-cool via the emission of synchrotron radiation. In a standard mixing cycle, antiprotons from three

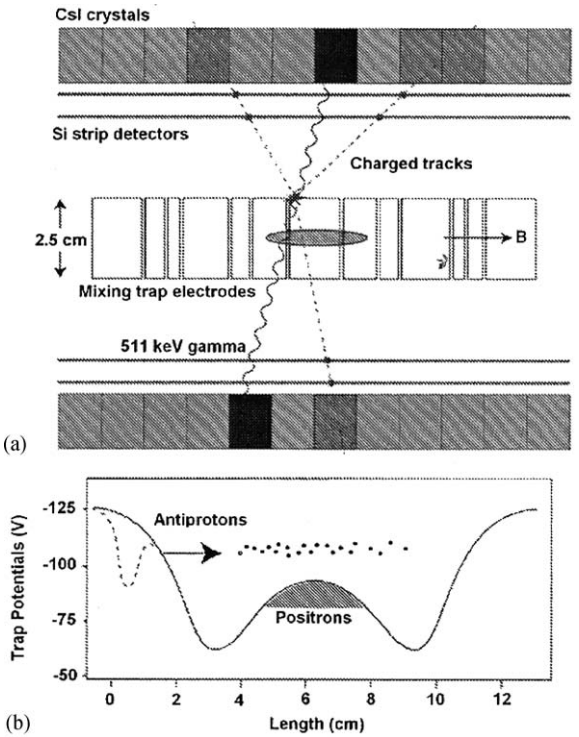

Fig. 2. (a) Schematic diagram, in axial section, of the ATHENA mixing trap and antihydrogen detector with a typical antihydrogen annihilation event. (b) The trapping potential on the axis of the mixing trap is plotted against length along the trap. The dashed line is the potential immediately before antiproton injection while the solid line is the potential during mixing.

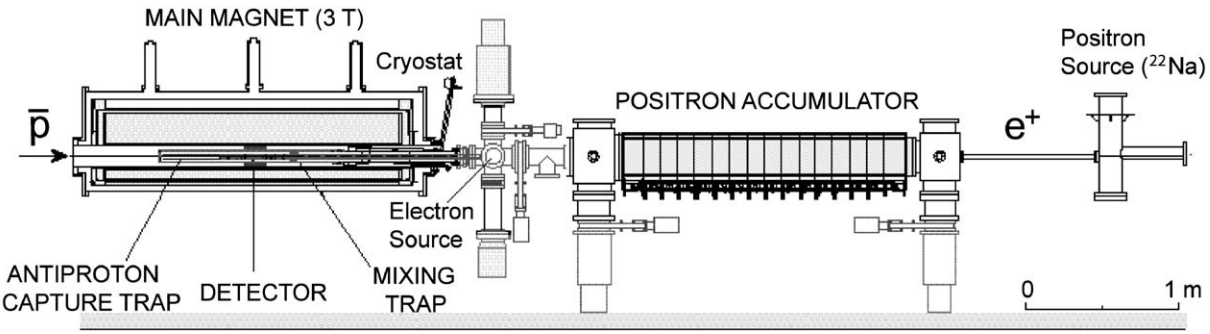

Fig. 1. Scheme of the ATHENA apparatus for the production and detection of antihydrogen.

AD spills are accumulated in the catching trap before they are transferred to the adjacent mixing trap. During the last data taking, about 10^4 antiprotons (per cycle) were transferred and used for mixing with positrons. In the near future, we plan to improve the transfer process in order to increase the number of antiprotons available for antihydrogen production.

Positrons are obtained from a radioactive source (1.7 GBq ^{22}Na) and are moderated by a frozen neon film. Their trapping and accumulation are achieved with the help of nitrogen buffer gas [6,7], which provides the dissipative process necessary for trapping the continuous flow of positrons. In the positron accumulator about 1.5×10^8 positrons are accumulated in cycles of roughly 5 min. They are then transferred into the mixing trap with an overall efficiency of about 50%; here, they reach a thermal equilibrium with the surrounding environment by synchrotron radiation in the 3 T field. The result is spheroidal positron plasma with a density of about ($1–2 \times 10^8$ cm^{-3}), a maximum length of about 3.4 cm and a typical radius of about 0.25 cm [8].

The technique used to mix the antiproton and positron clouds is based on the so-called ''nested'' potential configuration [9], which permits simultaneous confinement of oppositely charged particles (Fig. 2(b)). After the transfer of the two species in the mixing region, the antiprotons are injected into the positron plasma initiating the interaction process. An antiproton rapidly loses its energy via Coulomb collisions inside the positron plasma and eventually captures a positron producing an antihydrogen atom.

3. Antihydrogen detection

The formed atoms are neutral and they are not confined by the electromagnetic fields of the charged particle trap. They drift toward the walls and they are annihilated in the interaction with the matter (see Fig. 2(a)). Antihydrogen atoms are identified by detecting simultaneous annihilation (within ~ 5 μs) of antiprotons and positrons at the same place (vertex reconstruction $\sigma = \pm 4$ mm). Antiprotons annihilate into several charged or neutral particles (mostly pions), and the annihilation vertices are reconstructed by tracking the charged trajectories with two layers of double-sided silicon microstrip detectors. For each vertex, we search for clean evidence of 511 keV photons in the crystal data. A charged particle hit in a crystal, or an outer-layer silicon hit lying in the footprint of a crystal, excludes that particular crystal and its eight nearest neighbors. Next, we demand that exactly two of the remaining crystals have hits in an energy window around 511 keV, and that there are no hits of any energy adjacent to these two crystals. The energy calibration data, measured for each individual crystal, are used in this test. To search for antihydrogen in the sample of events having a vertex and two clean photons, we consider the opening angle, $\theta_{\gamma\gamma}$, between the lines connecting the vertex point to the geometric centers of the two hit crystals. For an antihydrogen event, this angle should be 180° (or $\cos(\theta_{\gamma\gamma}) = -1$). The opening angle distribution for reconstructed events detected during standard mixing cycles (also called ''cold mixing'' cycles) is shown in Fig. 3. For the real antihydrogen events, there should be a peak at $\cos(\theta_{\gamma\gamma}) \simeq -1$, and indeed this is what we experimentally observe.

The background was carefully studied in several ways. Measurements without positrons and only

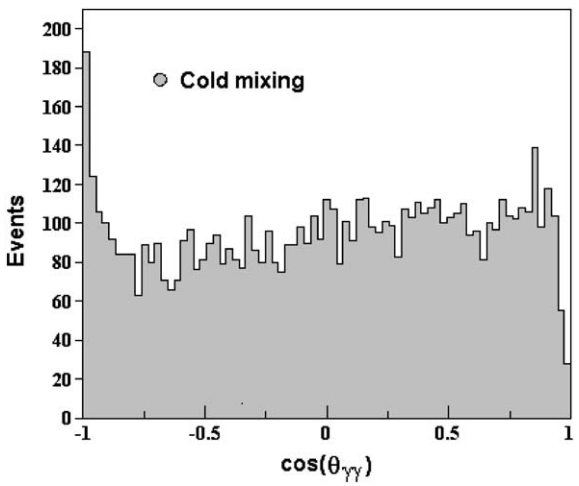

Fig. 3. Distribution of the opening angle between two 511 keV gamma rays, seen from the reconstructed vertices of antiproton annihilations in the case of antiproton mixing with cold. Figure from Ref. [1].

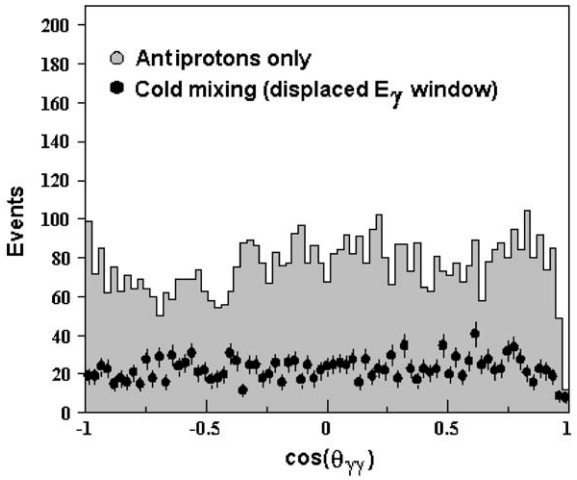

Fig. 4. The opening angle distribution (histogram) for antiproton-only data. The filled circles represent cold mixing data, analyzed using an energy (E_γ) window displaced upward so as not to include the 511 keV photo peak; no angular correlation of photons is seen. Figure from Ref. [1].

with antiprotons annihilated on the electrode wall were taken (Fig. 4: histogram). The storage time of the antiprotons without the interaction with the positrons can reach several hours [10] and we induce antiproton radial loss using different procedures, e.g. by injecting a low-energy (few tens of eV) electron beam throughout the antiproton cloud. In addition standard mixing data were analyzed with the gamma energy cut displaced (Fig. 4: circle). In both the background cases, no peak at $\cos(\theta_{\gamma\gamma}) \simeq -1$ is observed, as expected. Note that the three-dimensional imaging capability of the antiproton annihilation, as well as high angular resolution for gamma detection with segmented crystals, were essential in discriminating against the angular-uncorrelated gamma background, which comes predominantly from the decay and the subsequent electromagnetic shower of neutral pions. The neutral pions can produce secondary positrons (hence real 511 keV gammas) as well as higher-energy gammas.

4. Temperature-controlled production

An additional measurement of the background and a confirmation of the antihydrogen produc-

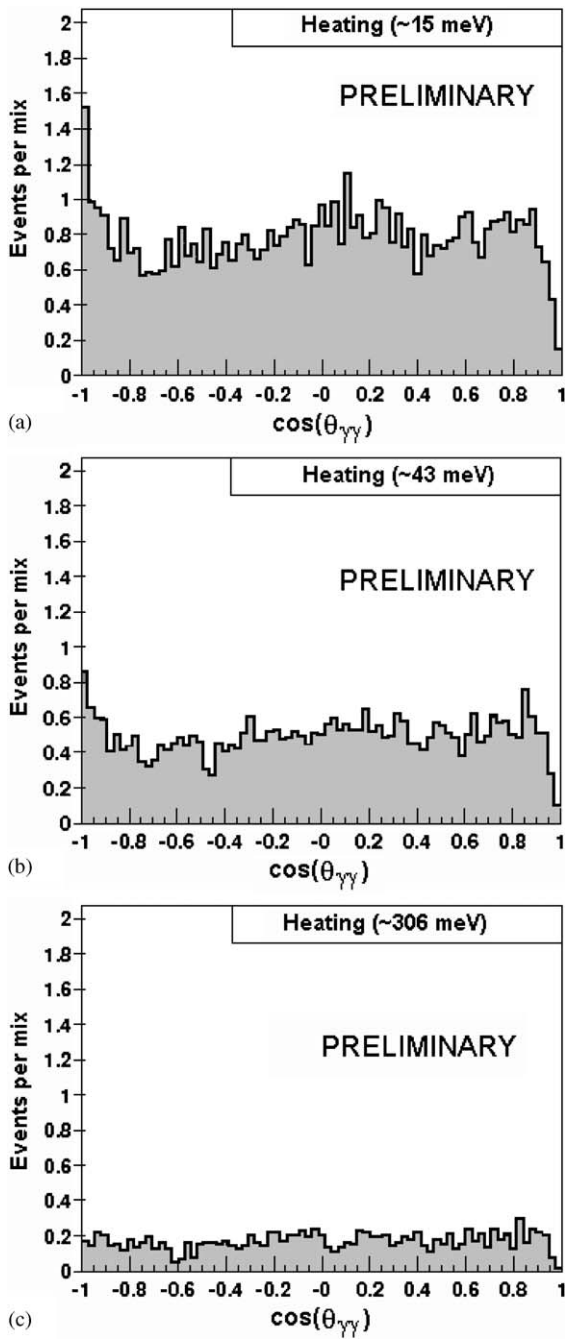

Fig. 5. Distribution of the opening angle cosine for antiproton mixing with RF-heated positron plasmas. The increases in the positron temperature are about (a) 15 meV, (b) 43 meV, and (c) 306 meV. All statistics are scaled to one single mixing cycle. The figure is obtained using all the collected statistics during 2003 data taken.

tion was obtained mixing antiprotons with a cloud of "hot" positrons. The temperature of the positron plasma was increased applying a radio-frequency (RF) signal [8]. Different RF heating powers were applied and we collected high statistics samples for three different increases of the plasma temperature: ~ 15 meV (~ 175 K), ~ 43 meV (~ 500 K); ~ 306 meV (~ 3500 K, also called "hot mixing"). The opening angle distributions for the three different increments are shown in Fig. 5. An increase in the positron temperature results in a progressive reduction of the peak at $\cos(\theta_{\gamma\gamma}) \simeq -1$, until the antihydrogen formation is completely turned off in the hot mixing case.

The collected data are the first measurements of the dependence of the antihydrogen formation on the positron plasma temperature. Since the two main recombination mechanisms (radiative and three-body [4]) have a different dependence on the temperature, detailed analysis on these data can give an insight into the production mechanism of the antiproton–positron combination.

5. Conclusions

In this article, we have briefly reviewed the first production and detection of antihydrogen by the ATHENA collaboration. Beyond this result, the ATHENA apparatus has allowed a variety of studies using cold antihydrogen; here we have also lightly touched upon the temperature dependence of the formation. This aspect together with other aspects like temporal modulation of antihydrogen production, or antihydrogen emission angular distribution are currently under investigation and will be the subject of our forthcoming publications.

Acknowledgements

The authors acknowledge J. Rochet, S. Bricola, G. Sobrero, and P. Chiggiato for their valuable technical support, and CERN's PS and AD crew for providing the excellent antiproton beam. This work was supported by INFN (Italy), FAPERJ (Brasil), MEXT (Japan), SNF (Switzerland), NSRC (Denmark), EPSRC (UK), and European Union.

References

[1] M. Amoretti, et al., Nature 419 (2002) 456.
[2] S. Maury, Hyperfine Interactions 109 (1997) 43.
[3] G. Gabrielse, et al., Phys. Rev. Lett. 89 (2002) 213401.
[4] M.H. Holzscheiter, M. Charlton, Rep. Progr. Phys. 62 (1999) 1 and references therein.
[5] C. Regenfus, Nucl. Instr. and Meth. A 501 (2003) 65.
[6] T.J. Murphy, C.M. Surko, Phys. Rev. A 46 (1992) 5696.
[7] L.V. Jørgensen, et al., in: F. Anderegg, L. Schweikhard, C.F. Driscoll (Eds.), Non-Neutral Plasma Physics IV, American Institute of Physics, New York, 2002, p. 35.
[8] M. Amoretti, et al., Phys. Rev. Lett. 91 (2003) 055001.
[9] G. Gabrielse, S.L. Rolston, L. Haarsma, W. Kells, Phys. Lett. 129A (1998) 38.
[10] M.C. Fujiwara, et al., Hyperfine Interactions 138 (2001) 153.